Delft University of Technology

Regularized Capon Beamformer Using ℓ1-Norm Applied to Photoacoustic Imaging

Paridar, Roya; Mozaffarzadeh, Moein; Basij, Maryam; Mehrmohammadi, Mohammad; Orooji, Mahdi

DOI
10.1109/ULTSYM.2018.8579612

Publication date
2018

Document Version
Final published version

Published in
2018 IEEE International Ultrasonics Symposium, IUS 2018

Citation (APA)
Paridar, R., Mozaffarzadeh, M., Basij, M., Mehrmohammadi, M., & Orooji, M. (2018). Regularized Capon Beamformer Using ℓ1-Norm Applied to Photoacoustic Imaging. In K. Hashimoto , & C. Ruppel (Eds.), *2018 IEEE International Ultrasonics Symposium, IUS 2018* (Vol. 2018-October). [8579612] IEEE . https://doi.org/10.1109/ULTSYM.2018.8579612

Important note
To cite this publication, please use the final published version (if applicable).
Please check the document version above.

Copyright
Other than for strictly personal use, it is not permitted to download, forward or distribute the text or part of it, without the consent of the author(s) and/or copyright holder(s), unless the work is under an open content license such as Creative Commons.

Takedown policy
Please contact us and provide details if you believe this document breaches copyrights.
We will remove access to the work immediately and investigate your claim.

This work is downloaded from Delft University of Technology.
For technical reasons the number of authors shown on this cover page is limited to a maximum of 10.

Green Open Access added to TU Delft Institutional Repository

'You share, we take care!' – Taverne project

https://www.openaccess.nl/en/you-share-we-take-care

Otherwise as indicated in the copyright section: the publisher is the copyright holder of this work and the author uses the Dutch legislation to make this work public.

Regularized Capon Beamformer using ℓ_1-Norm Applied to Photoacoustic Imaging

Roya Paridar
Department of Biomedical Engineering
Tarbiat Modares University
Tehran, Iran
roya.paridar@modares.ac.ir

Moein Mozaffarzadeh
Department of Biomedical Engineering
Tarbiat Modares University
Tehran, Iran
Department of Acoustical Wavefield Imaging
Delft University of Technology
Delft, The Netherlands
m.mozaffarzadeh@tudelft.nl

Maryam Basij
Department of Biomedical Engineering
Wayne State University
Detroit, MI, USA
n_basij@wayne.edu

Mohammad Mehrmohammadi
Department of Biomedical Engineering
Wayne State University
Detroit, MI, USA
mehr@wayne.edu

Mahdi Orooji*
Department of Biomedical Engineering
Tarbiat Modares University
Tehran, Iran
morooji@modares.ac.ir

***Abstract*—Delay-and-Sum (DAS), as a non-adaptive beamforming method, is one of the most common algorithms used in Photoacoustic imaging due to its simple implementation. The results obtained from this algorithm suffer from low resolution and high sidelobes. The adaptive Minimum variance (MV) method improves the image quality compared to DAS in terms of resolution and contrast. In this paper, it is proposed to add a ℓ_1-norm regularization term to the conventional MV minimization problem and create a new sparse beamforming method, named Modified-Sparse-MV (MS-MV) algorithm. In fact, the sparsity of the output is forced to the beampattern by adding this new sparse added term, which results in more noise reduction and sidelobe suppression compared to MV. The minimization problem is convex, and therefore, it can be solved using an iterative algorithm. The results show that the proposed MS-MV method improves the signal-to-noise-ratio for about 5.36 dB and 6.44 dB compared to DAS and MV, respectively, for the designed wire phantom.**

***Index Terms*—Photoacoustic imaging, beamforming, minimum variance, ℓ_1-norm regularization.**

I. Introduction

Photoacoustic tomography (PAT) is a non-ionizing hybrid medical imaging modality that exploits the high contrast of optical modality and the good resolution of ultrasound (US) imaging [1], [2]. It has a wide range of preclinical and clinical applications, such as early detection of cancer, tumor detection, imaging the whole body of small animals and etc. [3]–[8]. In PAT, a short laser pulse is employed to illuminate the tissue. The thermoelastic expansion occurs following the optical energy absorption, which results in acoustic wave propagation outside the tissue [9], [10]. Ultrasonic transducers, on form of linear, arc or circular shape, are positioned around the surface of the tissue to receive the generated acoustic waves [11], [12]. An image reconstruction method is used to construct the spatial distribution map of the tissue from the detected acoustic waves [13], [14]. One of the most common algorithms used in PA and US image formation, is the non-adaptive Delay-and-Sum (DAS) beamformer due to its simple implementation. However, the quality of the reconstructed images obtained from this algorithm is not satisfying due to its wide mainlobe and high level of sidelobes [15]. Delay-multiply-and-Sum (DMAS), introduced by Matrone et al. [16], improves the reconstructed images in terms of resolution and contrast compared to DAS. Some other algorithms have been introduced to enhance the image quality in comparison with DMAS algortihm [17]–[19]. Adaptive beamformers are also used to construct the images in which the received signals are weighted proportional to their characteristics, and result in an improved image in terms of resolution and contrast compared to non-adaptive beamformers. One of the adaptive beamformers commonly used in Radar and PA imaging (PAI), is Minimum variance (MV) beamformer in which the off-axis signals contribution is rejected while the unit gain at the focal point remains unchanged [20]. Some modifications have been applied to MV beamformer to improve the image quality compared to MV [21]–[26].

In order to suppress the sidelobes more efficiently, sparse based methods have been extensively used in Radar and Sonar applications, in which a sparse constraint is added to the existing minimization problem. Sparse capon (SC) beamformer is a sparse-based algorithm in which a ℓ_p-regularization term is added to the MV minimization problem to efficiently reject the level of noise with the assumption of $p \leq 1$ [27]. Another sparse-based algorithm, named ℓ_1-regularization minimum absolute distortionless response (ℓ_1-MADR) is introduced, where a sparse constraint is added to

Authorized licensed use limited to: TU Delft Library. Downloaded on July 31,2020 at 09:13:25 UTC from IEEE Xplore. Restrictions apply.

the Minimum Dispersion Distortionless Response (MDDR) [28], results in an improved image in terms of noise reduction compared to MV, and it has been shown that this algorithm is robust against noise. Also, more sidelobe suppression has been achieved in comparison with MV due to the new added constraint which results in Mainlobe-to-Sidelobe Power Ratio (MSPR) maximization [29].

In this paper, it is proposed to add the ℓ_1-norm regularization term to the existing MV minimization problem in order to force the sparsity to the whole beampattern and improve the reconstructed images compared to MV beamformer. The optimum weight would be obtained using an iterative algorithm used in [28]. The proposed Modified-Sparse-MV (MS-MV) algorithm would enhance the images in terms of noise reduction and sidelobe suppression compared to the conventional MV beamformer due to the sparse constraint added to the MV minimization problem.

In the following, the MV beamformer is described in section II. The proposed method is introduced in section III. Finally, the experimental results and the conclusion are presented in section IV and V, respectively.

II. Background

A. Minimum variance beamformer

Consider a linear array sensor consisting of M elements. the output of the MV beamformed signal, $y(k)$, is expressed as follows:

$$y(k)=\sum_{m=1}^{M} w_m(k)x_m(k-\Delta_m(k)), \tag{1}$$

where Δ_m is the time delay, $x_m(k-\Delta_m(k))$ is the delayed received signal from m^{th} element, k is the time index and $w_m(k)$ is the calculated weight. Consider the array of weights, $W(k)=[w_1(k),w_2(k),\cdots,w_m(k)]^T$, and the array of delayed signals, $X(k)=[x_1(k-\Delta_1(k)),x_2(k-\Delta_2(k)),\cdots,x_M(k-\Delta_M(k))]^T$. Equation (1) can be written as below:

$$y(k)=W^H(k)X(k), \tag{2}$$

The optimum weight would be achieved from maximizing the signal-to-interference-plus-noise ratio (SINR), which is equivalent to the following minimization problem [30]:

$$\underset{W(k)}{min}\, W(k)^H R(k)W(k), \quad \text{s.t.} \quad W(k)^H a=1, \tag{3}$$

where $(.)^H$ denotes the conjugate transpose operator, a is the steering vector which is defined as a vector of ones, and $R(k)$ represents the spatial covariance matrix. The optimum weight is obtained from the following equation:

$$W(k)=\frac{R(k)^{-1}a}{a^H R(k)^{-1}a}. \tag{4}$$

Using MV beamformer, the image quality would be improved compared to non-adaptive beamformers, as mentioned before, since it calculates the weight in the way that the large sidelobes are steered in directions where the received energy is low [31]. In practical applications, obtaining the exact spatial covariance matrix is unavailable, and therefore, the spatial covariance matrix should be estimated. Spatial smoothing and temporal averaging over $2K+1$ samples can be used to achieve a good estimation of the covariance matrix [32]:

$$\begin{aligned}\hat{R}(k)=&\frac{1}{(2K+1)(M-L+1)}\\ &\times\sum_{n=-K}^{K}\sum_{l=1}^{M-L+1}\bar{X}_l(k+n)\bar{X}_l(k+n)^H,\end{aligned} \tag{5}$$

where $\hat{R}(k)$ is the estimated covariance matrix, L is the subarray length and $\bar{X}_l(k)=[x_l(k),x_{l+1}(k),\cdots,x_{l+L-1}(k)]^T$ is the delayed received signals corresponding to l^{th} subarray. In order to obtain a more robust estimation, Diagonal loading (DL) can be applied to the covariance matrix in which $\Delta.trace\{R\}$ is added to the diagonal of $\hat{R}(k)$. Note that Δ is constant and is usually much smaller than $\frac{1}{L}$ [33]. Replacing $R(k)$ by $\hat{R}(k)$ in (4), the output beamformed signal would be achieved as below:

$$\tilde{y}(k)=\frac{1}{M-L+1}\sum_{l=1}^{M-L+1}W(k)^H\bar{X}_l(k). \tag{6}$$

III. Proposed method

A. Modified Sparse-Minimum Variance beamforming method

In this paper, it is proposed to add a ℓ_1-norm regularization term to the MV minimization problem in order to force the sparsity to the whole beampattern and suppress the sidelobes more efficiently compared to the MV beamformer. The optimization problem is defined as follows:

$$\underset{W_{MS}}{min} \quad \left(W^H RW+\alpha\|X_T^H W\|_1\right), \quad \text{s.t.} \quad a^H W=1. \tag{7}$$

where $X_T=[\bar{X}_1,\bar{X}_2,\cdots,\bar{X}_{M+L-1}]$, α is the regularization parameter which determines the trade-off between the MV constraint and the new regularization term, and $||.||_1$ represents the ℓ_1-norm of a vector. Note that the ℓ_0-norm is an accurate metric of the sparsity. However, ℓ_0-norm constraint leads to a non-convex problem, and therefore, the new sparse added term is considered to be ℓ_1-norm to make the problem convex [34]. The new added term can be interpreted as the sparsity of the output beamformed signal which is forced to the whole beampattern. The problem can be solved efficiently using the existing MATLAB toolboxes, such as [35]. In this work, the problem is solved using an iterative algorithm. In the following, the problem solving procedure is explained.

B. Problem solving

Equation (7) is rewritten as below:

$$\begin{aligned}&\underset{W_{MS}}{min} \quad \left(W^H RW+\alpha\|\Phi X_T^H W\|^2\right),\\ &\text{s.t.} \quad a^H W_S=1.\end{aligned} \tag{8}$$

where:

$$\Phi=\text{diag}\left\{|X_T^H W(1)|^{-1/2},\cdots,|X_T^H W(N)|^{-1/2}\right\}. \tag{9}$$

Authorized licensed use limited to: TU Delft Library. Downloaded on July 31,2020 at 09:13:25 UTC from IEEE Xplore. Restrictions apply.

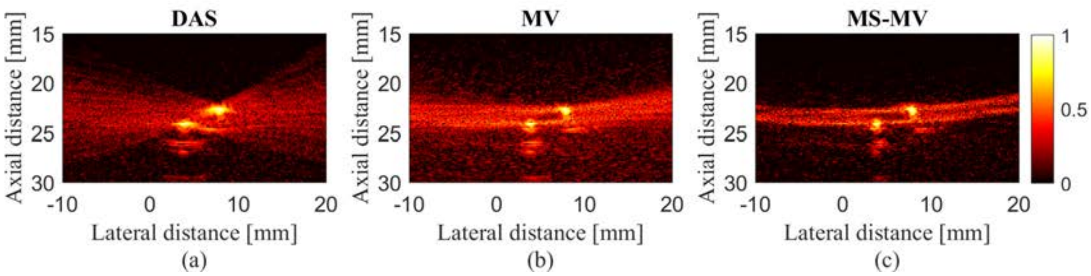

Fig. 1. The reconstructed experimental PA images using (a) DAS, (b) MV and (c) MS-MV. All the images are shown with a dynamic range of 50 dB. Two wires are used as the imaging target.

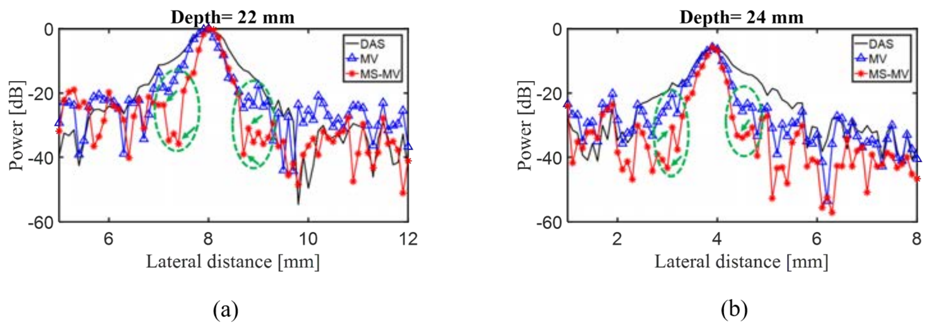

Fig. 2. The lateral variations of the reconstructed PA images shown in Fig. 1. Arrows and circles demonstrate the improvement caused by MS-MV algorithm.

With this new form of the minimization problem, the ℓ_1-norm form is converted into the ℓ_2-norm form, and therefore, the problem would be solved using Lagrangian multiplier method [34]. The optimum weight would be obtained from the following iterative method [24]:

$$W_{MS}^{k+1} = \frac{(R + \alpha X_T D(W^k) X_T^H)^{-1} a}{a^H (R + \alpha X_T D(W^k) X_T^H)^{-1} a}, \tag{10}$$

where $D(W) = \Phi^H \Phi$ and $(.)^k$ indicates $k^{th}(k = 0, 1, \cdots)$ step of the iteration procedure. Note that this algorithm is not sensitive to the initial weight. The iteration procedure continues until the calculated weights are converged, according to the following criteria:

$$\frac{1}{L} \left\| W_{MS}^{k+1} - W_{MS}^{k} \right\|^2 \leq \epsilon \tag{11}$$

IV. Results

A system consisting of an ultrasound data acquisition system, Vantage 128 Verasonics (Verasonics,Inc.,Redmond, WA) and a Q- switched Nd:YAG laser (EverGreen Laser, Double-pulse Nd: YAG system) is used for PAI. The pulse repetition rate of the laser is 25 Hz with 532 nm wavelength and 10 ns pulse width. A linear array sensor (L7-4, Philips Healthcare) consisting of 128 elements with 5.2 MHZ central frequency is used to receive the propagated PA waves from the designed phantom. A function generator is used to synchronize all operations (i.e., laser rings and PA signal recording). The data sampling rate is 20.8320 MHZ. It should be mentioned that the transducer is perpendicular to the wires. Thus, it is expected to see a cross section of the wires which would be similar to the point targets. Fig. 1 shows the reconstructed images of the designed wire phantom. It is obvious from the figures that the reconstructed image obtained from DAS results in a low resolution and high level of sidelobes. MV leads to image improvement in terms of resolution. However, the reconstructed image obtained from MV still suffers from high level of noise. The proposed MS-MV method, results in a high resolution while the sidelobes are suppressed more efficiently compared to MV, as shown in Fig. 1 (c). The lateral variations are presented in Fig. 2 in order to evaluate the beamformers in detail. It can be concluded that using the proposed MS-MV method, the resolution is improved compared to DAS beamformer, while more sidelobe suppression and noise reduction occurred compared to MV, as shown with the green circles and arrows in Fig. 2. Two quantitative evaluation metrics, Signal-to-noise-ratio (SNR) and Full-width-half-maximum ($FWHM$) are used to evaluate the beamformers quantitatively. MS-MV improves the SNR for about 7.29 dB and 3.43 dB at the depth of 22 mm and 24 mm, respectively, compared to DAS. Also, 7.86 dB and 5.03 dB SNR improvement occurs at the depth of 22 mm and 24 mm, respectively, in comparison with MV. The calculated $FWHM$s for different two depths are presented in TABLE I. It can be seen that the lowest value of $FWHM$ belongs to MS-MV, which indicates the resolution improvement compared to other beamformers.

V. Conclusion

It this paper, a new sparse beamforming method, named MS-MV was proposed, in which a ℓ_1-norm regularization

Authorized licensed use limited to: TU Delft Library. Downloaded on July 31,2020 at 09:13:25 UTC from IEEE Xplore. Restrictions apply.

TABLE I
THE CALCULATED $FWHM$ (mm) FOR THE DESIGNED WIRE PHANTOM.

Depth (mm)	DAS	MV	MS-MV
22	0.77	0.56	0.44
24	0.85	0.60	0.46

term was added to the MV minimization problem. This new sparse added term can be interpreted as the sparsity of the output that is forced to the whole beampattern, and leads to more noise reduction and sidelobe suppression compared to the conventional MV beamformer. The quantitative evaluation of the experimental results showed that the proposed MS-MV method leads to $FWHM$ improvement about 0.36 mm and 0.13 mm in average, compared to DAS and MV, respectively. Also, the calculated SNR was improved about 5.36 dB and 6.44 dB in average, compared to DAS and MV method, respectively, indicating the good performance of the proposed MS-MV method in contrast improvement.

REFERENCES

[1] B. Wang, L. Xiang, M. S. Jiang, J. Yang, Q. Zhang, P. R. Carney, and H. Jiang, "Photoacoustic tomography system for noninvasive real-time three-dimensional imaging of epilepsy," *Biomedical optics express*, vol. 3, no. 6, pp. 1427–1432, 2012.

[2] L. V. Wang, "Multiscale photoacoustic microscopy and computed tomography," *Nature photonics*, vol. 3, no. 9, p. 503, 2009.

[3] S. A. Ermilov, T. Khamapirad, A. Conjusteau, M. H. Leonard, R. Lacewell, K. Mehta, T. Miller, and A. A. Oraevsky, "Laser optoacoustic imaging system for detection of breast cancer," *Journal of biomedical optics*, vol. 14, no. 2, p. 024007, 2009.

[4] B. Guo, J. Li, H. Zmuda, and M. Sheplak, "Multifrequency microwave-induced thermal acoustic imaging for breast cancer detection," *IEEE Transactions on Biomedical Engineering*, vol. 54, no. 11, pp. 2000–2010, 2007.

[5] J. Xia and L. V. Wang, "Small-animal whole-body photoacoustic tomography: a review," *IEEE Transactions on Biomedical Engineering*, vol. 61, no. 5, pp. 1380–1389, 2014.

[6] M. Mehrmohammadi, S. Joon Yoon, D. Yeager, and S. Y Emelianov, "Photoacoustic imaging for cancer detection and staging," *Current molecular imaging*, vol. 2, no. 1, pp. 89–105, 2013.

[7] X. Wang, Y. Pang, G. Ku, X. Xie, G. Stoica, and L. V. Wang, "Noninvasive laser-induced photoacoustic tomography for structural and functional in vivo imaging of the brain," *Nature biotechnology*, vol. 21, no. 7, p. 803, 2003.

[8] S. Y. Nam and S. Y. Emelianov, "Array-based real-time ultrasound and photoacoustic ocular imaging," *Journal of the Optical Society of Korea*, vol. 18, no. 2, pp. 151–155, 2014.

[9] M. Jeon and C. Kim, "Multimodal photoacoustic tomography," *IEEE transactions on multimedia*, vol. 15, no. 5, pp. 975–982, 2013.

[10] M. Xu and L. V. Wang, "Photoacoustic imaging in biomedicine," *Review of scientific instruments*, vol. 77, no. 4, p. 041101, 2006.

[11] Y. Xu, D. Feng, and L. V. Wang, "Exact frequency-domain reconstruction for thermoacoustic tomography. i. planar geometry," *IEEE transactions on medical imaging*, vol. 21, no. 7, pp. 823–828, 2002.

[12] Y. Xu, M. Xu, and L. V. Wang, "Exact frequency-domain reconstruction for thermoacoustic tomography. ii. cylindrical geometry," *IEEE transactions on medical imaging*, vol. 21, no. 7, pp. 829–833, 2002.

[13] C.-W. Wei, T.-M. Nguyen, J. Xia, B. Arnal, E. Y. Wong, I. M. Pelivanov, and M. O'Donnell, "Real-time integrated photoacoustic and ultrasound (paus) imaging system to guide interventional procedures: ex vivo study," *IEEE transactions on ultrasonics, ferroelectrics, and frequency control*, vol. 62, no. 2, pp. 319–328, 2015.

[14] P. Omidi, M. Zafar, M. Mozaffarzadeh, A. Hariri, X. Haung, M. Orooji, and M. Nasiriavanaki, "A novel dictionary-based image reconstruction for photoacoustic computed tomography," *Applied Sciences*, vol. 8, no. 9, p. 1570, 2018.

[15] M. Mozaffarzadeh, V. Periyasamy, M. Pramanik, and B. Makkiabadi, "Efficient nonlinear beamformer based on pth root of detected signals for linear-array photoacoustic tomography: application to sentinel lymph node imaging," *Journal of Biomedical Optics*, vol. 23, no. 12, p. 121604, 2018.

[16] G. Matrone, A. S. Savoia, G. Caliano, and G. Magenes, "The delay multiply and sum beamforming algorithm in ultrasound b-mode medical imaging," *IEEE transactions on medical imaging*, vol. 34, no. 4, pp. 940–949, 2015.

[17] M. Mozaffarzadeh, A. Mahloojifar, M. Orooji, S. Adabi, and M. Nasiriavanaki, "Double-stage delay multiply and sum beamforming algorithm: Application to linear-array photoacoustic imaging," *IEEE Transactions on Biomedical Engineering*, vol. 65, no. 1, pp. 31–42, 2018.

[18] M. Mozaffarzadeh, M. Sadeghi, A. Mahloojifar, and M. Orooji, "Double-stage delay multiply and sum beamforming algorithm applied to ultrasound medical imaging," *Ultrasound in medicine & biology*, vol. 44, no. 3, pp. 677–686, 2018.

[19] M. Mozaffarzadeh, A. Hariri, C. Moore, and J. V. Jokerst, "The double-stage delay-multiply-and-sum image reconstruction method improves imaging quality in a led-based photoacoustic array scanner," *Photoacoustics*, vol. 12, pp. 22 – 29, 2018.

[20] J. Capon, "High-resolution frequency-wavenumber spectrum analysis," *Proceedings of the IEEE*, vol. 57, no. 8, pp. 1408–1418, 1969.

[21] S.-L. Wang and P.-C. Li, "Mvdr-based coherence weighting for high-frame-rate adaptive imaging," *IEEE transactions on ultrasonics, ferroelectrics, and frequency control*, vol. 56, no. 10, 2009.

[22] M. Mozaffarzadeh, Y. Yan, M. Mehrmohammadi, and B. Makkiabadi, "Enhanced linear-array photoacoustic beamforming using modified coherence factor," *Journal of biomedical optics*, vol. 23, no. 2, p. 026005, 2018.

[23] M. Mozaffarzadeh, A. Mahloojifar, V. Periyasamy, M. Pramanik, and M. Orooji, "Eigenspace-based minimum variance combined with delay multiply and sum beamformer: Application to linear-array photoacoustic imaging," vol. 25, pp. 1–8, IEEE, 2019.

[24] R. Paridar, M. Mozaffarzadeh, M. Mehrmohammadi, and M. Orooji, "Photoacoustic image formation based on sparse regularization of minimum variance beamformer," *Biomedical Optics Express*, vol. 9, no. 6, pp. 2544–2561, 2018.

[25] J. Li, X. Chen, Y. Wang, W. Li, and D. Yu, "Eigenspace-based generalized sidelobe canceler beamforming applied to medical ultrasound imaging," *Sensors*, vol. 16, no. 8, p. 1192, 2016.

[26] M. Mozaffarzadeh, A. Mahloojifar, M. Orooji, K. Kratkiewicz, S. Adabi, and M. Nasiriavanaki, "Linear-array photoacoustic imaging using minimum variance-based delay multiply and sum adaptive beamforming algorithm," *Journal of biomedical optics*, vol. 23, no. 2, p. 026002, 2018.

[27] Y. Zhang, B. Ng, and Q. Wan, "Sidelobe suppression for adaptive beamforming with sparse constraint on beam pattern," *Electronics Letters*, vol. 44, no. 10, pp. 615–616, 2008.

[28] X. Jiang, A. Yasotharan, and T. Kirubarajan, "Robust beamforming with sidelobe suppression for impulsive signals," *IEEE Signal Processing Letters*, vol. 22, no. 3, pp. 346–350, 2015.

[29] Y. Liu and Q. Wan, "Sidelobe suppression for robust capon beamforming with mainlobe-to-sidelobe power ratio maximization," *IEEE Antennas and Wireless Propagation Letters*, vol. 11, pp. 1218–1221, 2012.

[30] R. A. Monzingo and T. W. Miller, *Introduction to adaptive arrays*. Scitech publishing, 1980.

[31] J.-F. Synnevag, A. Austeng, and S. Holm, "Benefits of minimum-variance beamforming in medical ultrasound imaging," *IEEE transactions on ultrasonics, ferroelectrics, and frequency control*, vol. 56, no. 9, 2009.

[32] J.-F. Synnevåg, C.-I. Nilsen, and S. Holm, "P2b-13 speckle statistics in adaptive beamforming," in *Ultrasonics Symposium, 2007. IEEE*, pp. 1545–1548, IEEE, 2007.

[33] J. F. Synnevag, A. Austeng, and S. Holm, "Adaptive beamforming applied to medical ultrasound imaging," *IEEE transactions on ultrasonics, ferroelectrics, and frequency control*, vol. 54, no. 8, 2007.

[34] X. Jiang, W.-J. Zeng, A. Yasotharan, H.-C. So, and T. Kirubarajan, "Minimum dispersion beamforming for non-gaussian signals.," *IEEE Trans. Signal Processing*, vol. 62, no. 7, pp. 1879–1893, 2014.

[35] J. F. Sturm, "Using sedumi 1.02, a matlab toolbox for optimization over symmetric cones," *Optimization methods and software*, vol. 11, no. 1-4, pp. 625–653, 1999.

Authorized licensed use limited to: TU Delft Library. Downloaded on July 31,2020 at 09:13:25 UTC from IEEE Xplore. Restrictions apply.